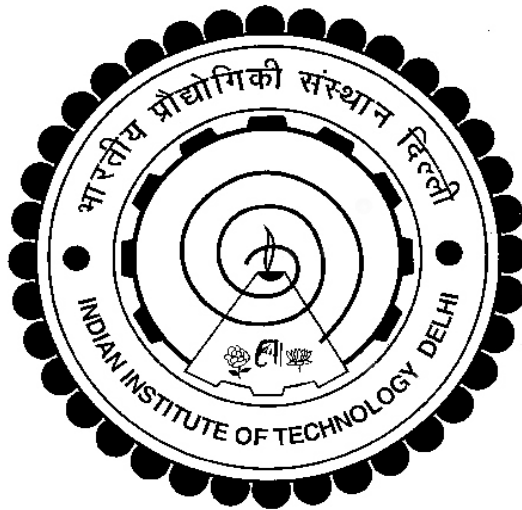


# **STRUCTURAL MECHANICS OF 3D WOVEN HONEYCOMB COMPOSITES**

**LEKHANI TRIPATHI**



**DEPARTMENT OF TEXTILE AND FIBRE ENGINEERING  
INDIAN INSTITUTE OF TECHNOLOGY DELHI**

**June 2023**

© Indian Institute of Technology Delhi (IITD), New Delhi, 2023

# **STRUCTURAL MECHANICS OF 3D WOVEN HONEYCOMB COMPOSITES**

by

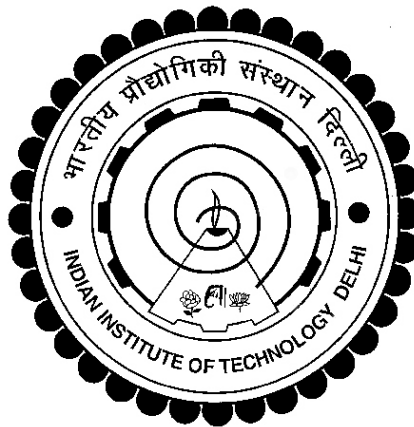
**LEKHANI TRIPATHI**

Department of Textile and Fibre Engineering

Submitted

in fulfilment of the requirement of the degree of Doctor of Philosophy

to the



**DEPARTMENT OF TEXTILE AND FIBRE ENGINEERING  
INDIAN INSTITUTE OF TECHNOLOGY DELHI**

June 2023

**Dedicated To My Parents**

## **CERTIFICATE**

This is to certify that the thesis entitled “**Structural mechanics of 3D woven honeycomb composites**” being submitted by **Ms. Lekhani Tripathi**, Entry No. **2018TTZ8454** to the Indian Institute of Technology Delhi for the award of the degree of **Doctor of Philosophy** is a record of bonafide research work carried out by her. Ms. Lekhani Tripathi has worked under my guidance and supervision. She has fulfilled all the requirements for the submission of this thesis. The results contained in this thesis have not been submitted, in part or full, to any other University or Institute for the award of any degree or diploma.

**Date:** 14/06/2023

**Place:** New Delhi

**Prof. B K Behera**

Department of Textile and Fibre Engineering

Indian Institute of Technology Delhi

New Delhi-110016

## **ACKNOWLEDGEMENTS**

Words of appreciation and gratitude fall short of acknowledging the inspiring guidance, valuable suggestions, and constant encouragement provided by Prof. B.K. Behera at every stage of this research. I enjoyed and learned a lot working under him throughout my Ph.D. I gratefully acknowledge the help and suggestions of my SRC members Prof. R. Alagirusamy, Prof. Samrat Mukhopadhyay, Prof. S. P. Singh (Department of Mechanical Engineering), and other faculty members of the department.

I acknowledge the help & cooperation of the lab staff, especially Mr. Vikas Khatkar, Mr. M. Kundu, and Mr. M. Singh, and I am thankful to all my friends, especially Mr. Gagandeep Singh Bhatia, Dr. Ghanshyam Neje, Dr. Zunjarrao Kamble, Dr. R.N. Manjunath, Mr. Soumya Chowdhury, Mr. Rupesh Ganvir, Dr. Meenakshi Ahirwar, Ms. Jaya Sharma, Ms. Shiwangi Shukla, Mr. Makhan Singh, Mr. Sandeep Olhan, Mr. Sameer Kumar Behera, Mr. Dushyant Dubey, Mr. Shubham Agnihotri and, Mr. Omender Kumar, for their help, support, and encouragement. At last, I would like to thank everyone who contributed directly or indirectly during my research work.

I express my sincere gratitude to my mother, father, brother, and friends for their motivation, moral support, and understanding.

**Date:** 14/06/2023

**Lekhani Tripathi**

**Place:** New Delhi

## Abstract

Honeycomb is considered an excellent structural material because of its high strength and shear rigidity, excellent energy absorbing property, high impact strength, lower weight, high crushing stress, and almost constant crushing force. Honeycomb being a cellular solid is a well-known core used to build sandwich structures while making structural composites. Because of this excellent mechanical performance, honeycombs are frequently used in the aircraft industry as a core of sandwich panels and in the automotive industry as efficient impact attenuators. The hollow spaces in the honeycomb structure reduce weight but also ensure the required strength, provided they are designed correctly. 3D woven honeycomb composite has a promising future in the lightweight application areas and can be the real substitute for aluminum and other metal alloys as these structures provide structural integrity. This thesis focuses on the manufacturing of lightweight 3D woven honeycomb composite structures of different cell geometry, the number of layers, face thickening sheet, honeycomb with different fibers, cell cross-sectional shape, different directions of hexagonal channels during weaving of honeycomb, and investigation of the effect of these parameters on the mechanical performance of their respective composites. Additionally, a comparison is made between the 3D woven honeycomb composite with metallic and 3D printed polymeric honeycomb composite structures of similar cell geometry with respect to their mechanical properties.

The textile fiber-based 3D woven honeycomb structure is engineered by using fabric geometrical parameters and mathematical expressions have been developed to calculate the repeat unit weight, fiber volume fraction (FVF), and specific weight of 3D woven honeycomb structures. Five 3D woven honeycomb fabric samples with different cell sizes of E-glass fiber were produced using model-based construction parameters on a customized rapier weaving machine. Fabric

dimensional parameters were determined experimentally to validate the model value with actual results. A reasonably high agreement was observed between experimental and theoretical values. This model can be used as a tool to engineer woven honeycomb reinforcement architecture to produce lightweight structural composite materials. The main objective of this section is to predict the weight of the repeat unit, FVF, and specific weight of the honeycomb structure with different cell geometrical parameters and different materials well before its production on the weaving machine.

In the next chapter, 3D woven honeycomb structures were developed with different cell geometry by varying the cell size, free wall length, bonded wall length, opening angle, and the number of honeycomb layers keeping overall composite thickness and cell shape constant. The variation of cell geometry was carried out by changing the number of picks in the honeycomb wall. Composite samples were prepared from the honeycomb preforms with epoxy resin (matrix) using VARIM (vacuum-assisted resin infusion method) process and characterized for their flatwise compression behavior. The results revealed that the structural parameters of the 3D woven honeycomb composite influenced flatwise compression energy significantly. The regular cell shape, smaller cell size, and higher number of layers of honeycomb composites exhibited higher specific energy absorption in flatwise compression. In edgewise compression and three-point bending analysis, the specific ultimate load is higher for a honeycomb composite structure with an opening angle of  $60^\circ$ , smaller cell sizes, small wall length, and for a higher number of layers keeping constant thickness or constant cell shape. In the low-velocity impact test, structural changes in honeycomb composite significantly affect the specific impact energy absorption. The specific impact energy absorption increases with large cell size, less opening angle, higher wall length, and a greater number of layers. The thickened face sheet was expected not to contribute to the compressive load

of the honeycomb structure; however, the bending load was improved consistently with the addition of each face sheet to the honeycomb core. 2LFC (Two-layer face sheet) has higher strength while with the increase in layer and also with 3D solid structure face sheet, specific compression energy decreased. An increase in face sheet thickness did not help to increase specific compression energy absorption but had a negative effect because of the increased weight and volume. The specific bending load was observed to be higher for 3D solid structure face sheet honeycomb composite as compared to 2D face sheet honeycomb composite of similar thickness.

3D woven honeycomb composites were prepared using three different fibers including natural and high-performance fibers to study the effect of fiber type on the mechanical properties of the honeycomb structure. The honeycomb fabric samples of similar areal density and cell size were produced from glass, sisal, and Kevlar fibers. The fabric samples were woven with similar free wall and bonded wall lengths by using a pre-decided number of picks. Other honeycomb cells parameters such as the height of the cell and the opening angle were kept constant by fabricating the moulds of the required dimension as per honeycomb cell size. Specific flatwise compression energy and specific ultimate load in edgewise compression was observed to be higher for Kevlar fiber composite as compared to glass, and sisal fiber composite. In the three-point bending and in-plane impact test, the Glass fiber honeycomb composite gives a higher specific bending load and impact energy compared to Kevlar and sisal honeycomb composites.

Numerical simulation along with experimental validation was used to investigate the flatwise compression behavior in the out-of-plane direction of 3D woven honeycomb composites with varied cell cross-sectional shapes such as hexagonal, triangular, and rectangular cell shapes. The total and unit cell perimeter of all three honeycomb cell shapes were kept constant to enable comparison of mechanical behavior. Edgewise compression, three-point bending behavior, and

impact energy were compared experimentally for all three configurations. The effect of cell cross-sectional shape on the mechanical properties of honeycomb composites was investigated. Among three honeycomb composites, hexagonal honeycomb gives superior mechanical performance. The flatwise compression behaviour of honeycomb structures has been predicted using FEM on the LS-DYNA platform, and the results have been validated using experimental data. The predicted values were in good agreement with the experimental results. Hexagonal honeycomb gives better flatwise compression energy as compared to other cell cross-sectional shapes as revealed by both experimental and numerical analysis.

The design and manufacturing of 3D woven honeycomb fabrics and their composites in both warp and weft directions were carried out to examine the effect of the direction of the hexagonal channel on the mechanical properties of the composites. Both the preforms were converted to their respective composites and mechanical analysis was carried out to understand the comparative advantage of the warp and weft way honeycomb weaving systems. The mechanical characteristics such as compression, three-point bending, and in-plane impact of composite samples were investigated keeping cell parameters constant. The comparison of mechanical properties of these two honeycomb composite samples revealed that warp-way honeycomb composites give better performance in edgewise compression and three-point bending test while weft-way honeycomb composite gives higher energy absorption under flatwise compression and high in-plane impact resistance. The direction of cell channels decides the direction of loading to the honeycomb cell. Since the crimps in the warp and weft directions are different, the deformation of honeycomb composite cells ought to be different in the warp and weft directions.

In the last chapter, the mechanical characteristics of 3D woven honeycomb composites were compared with the honeycomb of the existing technology of metallic honeycomb and polymeric

3D printed honeycomb. Mechanical characterization of aluminum honeycomb and 3D woven Kevlar honeycomb composite sandwich panels concerning their flatwise, edgewise compression, and three-point bending tests were carried out. 3D woven Kevlar honeycomb composite gives better results than the aluminum honeycomb for flatwise and three-point bending behavior. In the case of edgewise compression, aluminum honeycomb gives significant results as compared to 3D woven Kevlar honeycomb composite. The investigation of the mechanical behavior (i.e., compression, flexural, and impact) of FDM (fused deposition modelling)-built honeycomb structures and their comparison with 3D woven honeycomb composite structures were carried out. E-glass tow of 600 Tex was used to produce woven honeycomb samples. ABS (acrylonitrile butadiene styrene) was used as basic material to produce 3D printed honeycomb composite samples of identical cell geometry by the FDM process. The mechanical characterization revealed that the woven honeycomb structure gives better mechanical properties than the FDM-built honeycomb specimen. In flatwise compression, the FDM specimens give significant results as compared to woven honeycomb composites. However, other mechanical characteristics such as edgewise compression, three-point bending, and low-velocity impact behavior of woven honeycomb composites are superior to those of FDM specimens.

This research confirmed that the mechanical performance of 3D woven honeycomb composite structures is influenced by different parameters such as cell geometry, number of layers, face sheet thickening, fiber type, cell cross-sectional shape, and directions of hexagonal channels of honeycomb preform during weaving. The finding of this study can help to design and manufacture the honeycomb structures according to the end-use applications as it encompasses the detailed investigation of the mechanical performance of 3D woven honeycomb composites of different structural parameters. A comprehensive analysis of the relative advantage of honeycombs of

different manufacturing methods can be used as a suggestive guideline to select the appropriate technique based on mechanical performance, end-use applications, and cost of manufacturing.

## सार

हनीकॉम्ब को इसकी उच्च शक्ति और कतरनी कठोरता, उत्कृष्ट ऊर्जा अवशोषित संपत्ति, उच्च प्रभाव शक्ति, कम वजन, उच्च पेराई तनाव और लगभग निरंतर पेराई बल के कारण एक उत्कृष्ट संरचनात्मक सामग्री माना जाता है। हनीकॉम्ब एक सेलुलर ठोस होने के नाते एक प्रसिद्ध कोर है जिसका उपयोग संरचनात्मक कंपोजिट बनाते समय सैंडविच संरचनाओं के निर्माण के लिए किया जाता है। इस उत्कृष्ट यांत्रिक प्रदर्शन के कारण, विमान उद्योग में अक्सर सैंडविच पैनल के कोर के रूप में और मोटर वाहन उद्योग में कुशल प्रभाव क्षीणकों के रूप में हनीकॉम्ब का उपयोग किया जाता है। हनीकॉम्ब संरचना में खोखले स्थान वजन कम करते हैं लेकिन आवश्यक ताकत भी सुनिश्चित करते हैं, बशर्ते वे सही ढंग से डिजाइन किए गए हों। 3डी बुने हुए हनीकॉम्ब सम्मिश्र का हल्के अनुप्रयोग क्षेत्रों में एक आशाजनक भविष्य है और यह एल्यूमीनियम और अन्य धातु मिश्र धातुओं के लिए वास्तविक विकल्प हो सकता है क्योंकि ये संरचनाएं संरचनात्मक अखंडता प्रदान करती हैं। यह थीसिस विभिन्न सेल ज्यामिति के हल्के 3डी बुने हुए हनीकॉम्ब समग्र संरचनाओं के निर्माण, परतों की संख्या, फ़ेस शीट को मोटा करने वाली शीट, विभिन्न तंतुओं के साथ हनीकॉम्ब, सेल क्रॉस-अनुभागीय आकार, हनीकॉम्ब की बुनाई के दौरान हेक्सागोनल चैनलों की विभिन्न दिशाओं और जांच पर केंद्रित है। उनके संबंधित कंपोजिट के यांत्रिक प्रदर्शन पर इन मापदंडों के प्रभाव का। इसके अतिरिक्त, उनके यांत्रिक गुणों के संबंध में समान सेल ज्यामिति के धातु और 3 डी मुद्रित बहुलक हनीकॉम्ब समग्र संरचनाओं के साथ 3डी बुने हुए छत्ते के बीच तुलना की जाती है।

कपड़ा फाइबर आधारित 3डी बुनी हुई हनीकॉम्ब संरचना को कपड़े के ज्यामितीय मापदंडों का उपयोग करके इंजीनियर किया गया है और दोहराने वाली इकाई वजन, फाइबर वॉल्यूम अंश (एफवीएफ), और 3डी बुने हुए हनीकॉम्ब संरचनाओं के विशिष्ट वजन की गणना करने के लिए गणितीय अभिव्यक्ति विकसित की गई है। ई-ग्लास फाइबर के विभिन्न सेल आकारों के साथ पांच 3डी बुने हुए छत्ते के कपड़े के नमूने एक

अनुकूलित रेपियर बुनाई मशीन पर मॉडल-आधारित निर्माण मापदंडों का उपयोग करके तैयार किए गए थे। वास्तविक परिणामों के साथ मॉडल मूल्य को मान्य करने के लिए फैब्रिक डायमेंशनल पैरामीटर प्रयोगात्मक रूप से निर्धारित किए गए थे। प्रायोगिक और सैद्धांतिक मूल्यों के बीच यथोचित उच्च समझौता देखा गया। हल्के संरचनात्मक समग्र सामग्री का उत्पादन करने के लिए इस मॉडल को इंजीनियर बुने हुए हनीकॉम्ब सुट्टीकरण आर्किटेक्चर के उपकरण के रूप में उपयोग किया जा सकता है। इस खंड का मुख्य उद्देश्य बुनाई मशीन पर इसके उत्पादन से पहले विभिन्न सेल ज्यामितीय मापदंडों और विभिन्न सामग्रियों के साथ रिपीट यूनिट, एफवीएफ और हनीकॉम्ब संरचना के विशिष्ट वजन का अनुमान लगाना है।

अगले अध्याय में, सेल आकार, मुक्त दीवार की लंबाई, बंधी हुई दीवार की लंबाई, उद्घाटन कोण, और समग्र समग्र मोटाई और सेल आकार को स्थिर रखते हुए छत्ते की परतों की संख्या को अलग-अलग सेल ज्यामिति के साथ 3 डी बुने हुए हनीकॉम्ब संरचनाओं को विकसित किया गया था। हनीकॉम्ब की दीवार में पिक्स की संख्या को बदलकर सेल ज्यामिति की भिन्नता को अंजाम दिया गया। VARIM (वैक्यूम-असिस्टेड रेजिन इन्फ्यूजन मेथड) प्रक्रिया का उपयोग करके एपॉक्सी राल (मैट्रिक्स) के साथ छत्ते के प्रीफॉर्म से समग्र नमूने तैयार किए गए और उनके फ्लैटवाइज संपीड़न व्यवहार की विशेषता बताई गई। परिणामों से पता चला कि 3डी बुने हुए हनीकॉम्ब सम्मिश्र के संरचनात्मक मापदंडों ने फ्लैटवाइज संपीड़न ऊर्जा को महत्वपूर्ण रूप से प्रभावित किया। नियमित सेल आकार, छोटे सेल आकार, और हनीकॉम्ब कंपोजिट की उच्च संख्या में परतों ने फ्लैटवाइज संपीड़न में उच्च विशिष्ट ऊर्जा अवशोषण प्रदर्शित किया। एजवाइज कम्प्रेसन और थ्री-पॉइंट बेंडिंग एनालिसिस में, 60 डिग्री के ओपनिंग एंगल, छोटे सेल साइज, छोटी दीवार की लंबाई और लगातार मोटाई या स्थिर सेल रखने वाली परतों की उच्च संख्या के साथ हनीकॉम्ब कम्पोजिट स्ट्रक्चर के लिए विशिष्ट अंतिम भार अधिक होता है। आकार। कम-वेग प्रभाव परीक्षण में, हनीकॉम्ब समग्र में संरचनात्मक परिवर्तन विशिष्ट प्रभाव ऊर्जा अवशोषण को महत्वपूर्ण रूप से प्रभावित करते हैं। विशिष्ट प्रभाव ऊर्जा अवशोषण बढ़े

सेल आकार, कम उद्घाटन कोण, उच्च दीवार की लंबाई और अधिक संख्या में परतों के साथ बढ़ता है। मोटी शीट से छत्ते की संरचना के संपीड़ित भार में योगदान नहीं करने की उम्मीद की गई थी, हालांकि, प्रत्येक चेहरे की शीट को हनीकॉम्ब कोर में जोड़ने के साथ झुकने वाले भार में लगातार सुधार हुआ था। 2LFC (टू-लेयर फेस शीट) में उच्च शक्ति है जबकि परत में वृद्धि के साथ और 3D ठोस संरचना फेस शीट के साथ, विशिष्ट संपीड़न ऊर्जा में कमी आई है। फेस शीट की मोटाई में वृद्धि ने विशिष्ट संपीड़न ऊर्जा अवशोषण को बढ़ाने में मदद नहीं की, लेकिन वजन और मात्रा में वृद्धि के कारण इसका नकारात्मक प्रभाव पड़ा। समान मोटाई के 2डी फेस शीट हनीकॉम्ब कम्पोजिट की तुलना में 3डी सॉलिड स्ट्रक्चर फेस शीट हनीकॉम्ब कम्पोजिट के लिए विशिष्ट बेंडिंग लोड अधिक पाया गया।

हनीकॉम्ब संरचना के यांत्रिक गुणों पर फाइबर प्रकार के प्रभाव का अध्ययन करने के लिए प्राकृतिक और उच्च-प्रदर्शन फाइबर सहित तीन अलग-अलग फाइबर का उपयोग करके 3डी बुने हुए हनीकॉम्ब कंपोजिट तैयार किए गए थे। समान क्षेत्र घनत्व और कोशिका आकार के हनीकॉम्ब के कपड़े के नमूने का गिलास, सिसल और केवलर फाइबर से निर्मित किए गए थे। कपड़े के नमूने समान मुक्त दीवार और बंधी हुई दीवार की लंबाई के साथ पूर्व-निर्धारित संख्या में पिक्स का उपयोग करके बुने गए थे। अन्य हनीकॉम्ब कोशिकाओं के मापदंडों जैसे कि कोशिका की ऊंचाई और उद्घाटन कोण को छत्ते के आकार के अनुसार आवश्यक आयाम के सांचों को बनाकर स्थिर रखा गया था। ग्लास और सिसल फाइबर कम्पोजिट की तुलना में केवलर फाइबर कम्पोजिट के लिए विशिष्ट फ्लैटवाइज कंप्रेशन एनर्जी और एजवाइज कंप्रेशन में विशिष्ट अंतिम भार अधिक पाया गया। थ्री-पॉइंट बेंडिंग और इन-प्लेन इम्पैक्ट टेस्ट में, ग्लास फाइबर हनीकॉम्ब कम्पोजिट केवलर और सिसल हनीकॉम्ब कंपोजिट की तुलना में उच्च विशिष्ट झुकने वाला भार और प्रभाव ऊर्जा देता है।

प्रयोगात्मक सत्यापन के साथ संख्यात्मक सिमुलेशन का उपयोग हेक्सागोनल, त्रिकोणीय और आयताकार सेल आकृतियों जैसे विभिन्न सेल क्रॉस-अनुभागीय आकृतियों के साथ 3डी बुने हुए हनीकॉम्ब कंपोजिट के

आउट-ऑफ-प्लेन दिशा में फ्लैटवाइज संपीडन व्यवहार की जांच के लिए किया गया था। यांत्रिक व्यवहार की तुलना को सक्षम करने के लिए सभी तीन हनीकॉम्ब सेल आकृतियों की कुल और इकाई सेल परिधि को स्थिर रखा गया था। तीनों विन्यासों के लिए समान रूप से संपीडन, तीन-बिंदु झुकने वाला व्यवहार और प्रभाव ऊर्जा की प्रयोगात्मक रूप से तुलना की गई थी। हनीकॉम्ब कंपोजिट के यांत्रिक गुणों पर सेल क्रॉस-सेक्शनल आकार के प्रभाव की जांच की गई। तीन हनीकॉम्ब सम्मिश्रणों में, हेक्सागोनल हनीकॉम्ब बेहतर यांत्रिक प्रदर्शन देता है। एलएस-डीवाईएनए प्लेटफॉर्म पर एफईएम का उपयोग करके हनीकॉम्ब संरचनाओं के फ्लैटवाइज संपीडन व्यवहार की भविष्यवाणी की गई है, और प्रयोगात्मक डेटा का उपयोग करके परिणामों को मान्य किया गया है। प्रायोगिक परिणामों के साथ अनुमानित मूल्य अच्छे समझौते में थे। हेक्सागोनल हनीकॉम्ब अन्य सेल क्रॉस-सेक्शनल आकृतियों की तुलना में बेहतर सपाट संपीडन ऊर्जा देता है जैसा कि प्रायोगिक और संख्यात्मक विश्लेषण दोनों से पता चलता है।

कंपोजिट के यांत्रिक गुणों पर हेक्सागोनल चैनल की दिशा के प्रभाव की जांच करने के लिए 3डी बुने हुए हनीकॉम्ब के कपड़े और ताना और बाना दोनों दिशाओं में उनके कंपोजिट का डिजाइन और निर्माण किया गया। दोनों प्रीफॉर्म्स को उनके संबंधित कंपोजिट में परिवर्तित किया गया था और ताने और बाने के तरीके हनीकॉम्ब बुनाई प्रणालियों के तुलनात्मक लाभ को समझने के लिए यांत्रिक विश्लेषण किया गया था। सेल मापदंडों को स्थिर रखते हुए यांत्रिक विशेषताओं जैसे संपीडन, तीन-बिंदु झुकने और मिश्रित नमूनों के इन-प्लेन प्रभाव की जांच की गई। इन दो हनीकॉम्ब सम्मिश्रण नमूनों के यांत्रिक गुणों की तुलना से पता चला है कि वार्प-वे हनीकॉम्ब सम्मिश्रण एजवाइज संपीडन और तीन-बिंदु झुकने परीक्षण में बेहतर प्रदर्शन देते हैं जबकि वेप्ट-वे हनीकॉम्ब सम्मिश्रण फ्लैटवाइज संपीडन और उच्च इन-प्लेन प्रभाव प्रतिरोध के तहत उच्च ऊर्जा अवशोषण देता है। . सेल चैनलों की दिशा हनीकॉम्ब सेल को लोड करने की दिशा तय करती है। चूँकि ताने

और बाने की दिशाओं में ऐंठन अलग-अलग होती है, ताने और बाने की दिशाओं में हनीकॉम्ब मिश्रित कोशिकाओं की विकृति अलग-अलग होनी चाहिए।

पिछले अध्याय में, 3डी बुने हुए हनीकॉम्ब कंपोजिट की यांत्रिक विशेषताओं की तुलना धात्विक हनीकॉम्ब और बहुलक 3डी मुद्रित छत्ते की मौजूदा तकनीक के छत्ते से की गई थी। एल्यूमीनियम हनीकॉम्ब और 3डी बुने हुए केवलर हनीकॉम्ब मिश्रित सैंडविच पैनल के यांत्रिक लक्षण वर्णन उनके फ्लैटवाइज, किनारे की दिशा में संपीड़न, और तीन-बिंदु झुकने वाले परीक्षण किए गए। 3डी बुना हुआ केवलर हनीकॉम्ब सम्मिश्र सपाट और तीन-बिंदु झुकने वाले व्यवहार के लिए एल्यूमीनियम हनीकॉम्ब की तुलना में बेहतर परिणाम देता है। किनारे के अनुसार संपीड़न के मामले में, 3डी बुने हुए केवलर हनीकॉम्ब सम्मिश्र की तुलना में एल्यूमीनियम हनीकॉम्ब महत्वपूर्ण परिणाम देता है। एफडीएम (फ्यूज डिपोजिशन मॉडलिंग) निर्मित हनीकॉम्ब संरचनाओं के यांत्रिक व्यवहार (यानी, संपीड़न, फ्लेक्सुरल और प्रभाव) की जांच और 3डी बुने हुए हनीकॉम्ब समग्र संरचनाओं के साथ उनकी तुलना की गई। बुने हुए छत्ते के नमूनों का उत्पादन करने के लिए 600 टेक्स के ई-ग्लास टो का उपयोग किया गया था। FDM प्रक्रिया द्वारा समान सेल ज्यामिति के 3D मुद्रित छत्ते के मिश्रित नमूनों का उत्पादन करने के लिए ABS (एक्रिलोनिट्राइल ब्यूटाडाइन स्टाइरीन) का उपयोग मूल सामग्री के रूप में किया गया था। यांत्रिक लक्षण वर्णन से पता चला है कि बुना हुआ हनीकॉम्ब संरचना एफडीएम-निर्मित छत्ते के नमूने की तुलना में बेहतर यांत्रिक गुण देता है। फ्लैटवाइज कम्प्रेसन में, FDM नमूने बुने हुए हनीकॉम्ब कंपोजिट की तुलना में महत्वपूर्ण परिणाम देते हैं। हालांकि, अन्य यांत्रिक विशेषताएं जैसे कि एडगेवाइज कम्प्रेसन, थ्री-पॉइंट बेंडिंग, और बुने हुए हनीकॉम्ब कंपोजिट के कम-वेग प्रभाव व्यवहार FDM नमूनों से बेहतर हैं।

इस शोध ने पुष्टि की कि 3डी बुने हुए हनीकॉम्ब समग्र संरचनाओं का यांत्रिक प्रदर्शन विभिन्न मापदंडों से प्रभावित होता है जैसे कि सेल ज्यामिति, परतों की संख्या, चेहरे की शीट का मोटा होना, फाइबर प्रकार, सेल क्रॉस-अनुभागीय आकार, और बुनाई के दौरान छत्ते के हेक्सागोनल चैनलों की दिशाएं . इस अध्ययन की खोज अंत-उपयोग अनुप्रयोगों के अनुसार हनीकॉम्ब संरचनाओं को डिजाइन और निर्माण करने में मदद कर सकती है क्योंकि इसमें विभिन्न संरचनात्मक मापदंडों के 3डी बुने हुए हनीकॉम्ब कंपोजिट के यांत्रिक प्रदर्शन की विस्तृत जांच शामिल है। विभिन्न निर्माण विधियों के छत्ते के सापेक्ष लाभ का एक व्यापक विश्लेषण यांत्रिक प्रदर्शन, अंतिम उपयोग अनुप्रयोगों और निर्माण की लागत के आधार पर उपयुक्त तकनीक का चयन करने के लिए एक सुझावात्मक दिशानिर्देश के रूप में उपयोग किया जा सकता है।

# Contents

	<b>Page No.</b>
Certificate	i
Acknowledgements	ii
Abstract	iii
Table of Contents	xv
List of Figures	xxiv
List of Tables	xxxix
List of Abbreviations	xli
<b>Chapter 1: Introduction</b>	<b>1</b>
1.1 Background	1
1.2 Motivation	5
<b>Chapter 2: Research objectives</b>	<b>8</b>
2.1 Principal objective	8
2.2 Sub-objectives	8
<b>Chapter 3: Literature review</b>	<b>9</b>
3.1 Introduction	9
3.2 Cellular structure	10
3.2.1 Manmade cellular materials	10
3.3 Honeycomb structure	13
3.3.1 Honeycomb as a core of the sandwich structure	15
3.3.2 Manufacturing of honeycomb structure	19
3.4 Energy absorption of cellular solids	22
3.4.1 Mathematical modelling for the elastic buckling of honeycomb	23
3.4.1.1 Evaluating the value of stress	24
3.4.1.2 Derivation of buckling formula	25
3.5 Three – dimensional woven fabric	27
3.5.1 3D woven hollow spacer structures	31

	<b>Page No.</b>
3.5.2 Classification of honeycomb weave	32
3.5.2.1 2D honeycomb weave	32
3.5.2.2 3D woven honeycomb fabric	34
3.6 Textile honeycomb composite	36
3.7 Geometrical modelling of repeat unit cell of 3D woven honeycomb structures	37
3.8 FEM (finite element modelling) analysis	38
3.9 Properties of the honeycomb structure	42
3.9.1 Stiffness and strength of honeycomb structure	44
3.9.2 Crushing and compression behaviour of honeycomb structure	45
3.9.3 Impact behavior of honeycomb structure	51
3.9.4 Bending behavior of honeycomb	56
3.10 Influence of structural parameters on mechanical properties	58
3.11 Application of honeycomb structures	61
3.11.1 Prominent current applications	62
3.12 Auxetic Honeycomb	64
3.13 Comparison of Metal based with composites-based structure	68
<b>Chapter 4: Materials and Methods</b>	<b>70</b>
4.1 Introduction	70
4.2 Materials	71
4.2.1 Glass Fibers	71
4.2.2 Aramid Fibers	71
4.2.3 Sisal Fiber	72
4.2.4 Epoxy resin	73
4.2.5 Aradur HY 951 Hardener	74
4.2.6 ABS (acrylonitrile butadiene styrene)	75
4.2.7 Aluminum honeycomb	76
4.3 Methods	77

	<b>Page No.</b>
4.3.1 Optimization of pre-treatment of natural fiber	77
4.3.1.1 Alkali treatment	77
4.3.2 Representation of 3D woven honeycomb structure	77
4.3.3 Weave architecture of 3D woven honeycomb fabric	79
4.3.4 Calculation for design parameters of honeycomb fabric	80
4.3.5 Production of 3D woven honeycomb fabric	81
4.3.6 Geometrical modelling of repeat unit cell of 3D woven honeycomb structures	83
4.3.7 Production of 3D woven honeycomb composites	83
4.3.8 Mechanical characterization	86
4.3.8.1 Characterization for flatwise compressive properties	86
4.3.8.1.1 Determination of specific compression energy	87
4.3.8.2 Characterization for edgewise compressive properties	88
4.3.8.2.1 Determination of specific load for edgewise compression	89
4.3.8.3 Characterization for three-point bending Properties	89
4.3.8.3.1 Determination of specific load for three- point bending	90
4.3.8.4 Characterization for Drop weight impact test	91
4.3.8.4.1 Determination of impact properties under in- plane impact loading	92
<b>Chapter 5: To develop a geometrical model of 3D woven honeycomb structure to determine fiber volume fraction (FVF), repeat unit weight, and specific weight of the fabric to enable calculation of woven construction parameters</b>	93
5.1 Introduction	93
5.2 Materials	96
5.3 Methodology	96
5.3.1 Production of 3D woven honeycomb fabric	96

	<b>Page No.</b>
5.3.2 Modelling Approach	100
5.3.2.1 Input Parameters	101
5.3.2.2 Output parameters	102
5.4 Results and Discussion	106
5.4.1 Comparison of predicted and experimental geometrical parameters	106
5.4.2 Prediction of repeat unit weight, FVF, and specific weight	109
5.5 Conclusions	114
<b>Chapter 6: Development and characterization of 3D woven honeycomb composites with different cell geometry, number of layers and face-thickening sheet</b>	<b>116</b>
6.1 Introduction	116
6.2 Materials	120
6.3 Methodology	121
6.3.1 Experimental design outline for different cell geometrical parameters	121
6.3.2 Production of 3D woven honeycomb fabric	126
6.3.3 Production of 3D woven honeycomb composite	135
6.3.4 Experimental design outline for different face thickening sheets	138
6.3.4.1 Production of 2D plain and 3D orthogonal fabric and their composites for face sheets	139
6.3.5 Mechanical characterization of 3D woven honeycomb composites	142
6.4 Results and discussion	143
6.4.1 Flatwise compression	143
6.4.1.1 Variation of Cell size	143
6.4.1.2 Variation of Opening angle	145
6.4.1.3 Variation of free wall length	146
6.4.1.4 Variation of bonded wall length	148

	<b>Page No.</b>
6.4.1.5 Variation in the number of layers keeping the thickness of composite constant	150
6.4.1.6 Variation in the number of layers keeping cell shape constant	151
6.4.1.7 Effect of face thickening sheets	153
6.4.2 Edgewise compression	157
6.4.2.1 Variation of Cell size	157
6.4.2.2 Variation of Opening angle	158
6.4.2.3 Variation of free wall length	160
6.4.2.4 Variation of bonded wall length	162
6.4.2.5 Variation in the number of layers keeping cell shape constant	163
6.4.2.6 Variation in the number of layers keeping the thickness of composite constant	165
6.4.3 Three-point bending	168
6.4.3.1 Variation of Cell size	168
6.4.3.2 Variation of Opening angle	170
6.4.3.3 Variation of free wall length	172
6.4.3.4 Variation of bonded wall length	173
6.4.3.5 Variation in the number of layers keeping cell shape constant	175
6.4.3.6 Variation in the number of layers keeping the thickness of composite constant	176
6.4.3.7 Effect of face thickening sheets	178
6.4.4 Low-velocity in-plane impact energy	183
6.4.4.1 Effect of cell size on impact behavior	183
6.4.4.2 Effect of Opening angle on impact behavior	185
6.4.4.3 Effect of free wall length on impact behavior	187
6.4.4.4 Effect of bonded wall length on impact behavior	188

	<b>Page No.</b>
6.4.4.5 Effect of the number of layers keeping the thickness of composite constant on impact behavior	190
6.4.4.6 Effect of the number of layers keeping cell shape constant on impact behavior	192
6.5 Conclusions	194
<b>Chapter 7: To develop and characterize 3D woven honeycomb composites with different types of fibers.</b>	<b>196</b>
7.1 Introduction	196
7.2 Materials	199
7.3 Methodology	199
7.3.1 Production of 3D woven honeycomb fabrics and their composites	199
7.3.2 Mechanical characterization of 3D woven honeycomb composites	203
7.4 Results and discussions	204
7.4.1 Flatwise compression	204
7.4.2 Edgewise compression	206
7.4.3 Three-point bending	208
7.4.4 Low-velocity in-plane impact energy	210
7.5 Conclusions	212
<b>Chapter 8: Modelling and experimental validation of flatwise compression energy of 3D woven honeycomb composites with different cell cross-sectional shapes</b>	<b>213</b>
8.1 Introduction	213
8.2 Materials	215
8.3 Methodology	215
8.3.1 Calculation of the total perimeter of the different honeycomb structures	216
8.3.2 Calculation of mass of the different structures	217
8.3.3 Fabrication of 3D honeycomb fabric	218

	<b>Page No.</b>
8.3.4 Production of the 3D woven honeycomb composite	219
8.3.5 Prediction of compression energy of unit cell of honeycomb composite by FEM analysis	220
8.3.5.1 Honeycomb model development in SOLIDWORKS Platform	221
8.3.5.2 Fiber parameter determination for model preparation	221
8.3.5.3 Numerical Modelling	222
8.3.5.4 Material Property	222
8.3.5.5 Honeycomb structure with different cell geometry other than the hexagon	223
8.3.6 Mechanical characterization of honeycomb composites	224
8.4 Results and Discussion	224
8.4.1 Mechanical behavior of different cell structures	224
8.4.2 Analysis of the failure mechanism of different cell structures	229
8.4.2.1 Flatwise compression	229
8.4.2.2 Edgewise compression	230
8.4.2.3 Three-point bending	231
8.4.2.4 Low-velocity in-plane impact behavior	231
8.4.3 Comparison of the simulated results with experimental values for model validation	232
8.5 Conclusions	237
<b>Chapter 9: Comparative analysis of mechanical behavior of 3D woven honeycomb composites produced in warp and weft directions</b>	<b>238</b>
9.1 Introduction	238
9.2 Materials	240
9.3 Methodology	240
9.3.1 Weave architecture of 3D woven honeycomb fabric	240
9.3.2 Fabrication of 3D woven honeycomb fabric	241
9.3.3 Composite processing	247
9.3.4 Characterization of honeycomb composites	248

	<b>Page No.</b>
9.4 Results and Discussion	249
9.4.1 Flatwise compression	249
9.4.2 Edgewise compression	251
9.4.3 Three-point bending	253
9.4.4 Low-velocity in-plane impact energy	255
9.5 Conclusions	258
<b>Chapter 10: To compare the mechanical performance of 3D woven honeycomb composite with that of metallic honeycomb and 3D printed polymeric honeycomb composites of similar cell geometry</b>	259
10.1 Comparative analysis of the mechanical properties of Aluminum core honeycomb with 3D woven Kevlar honeycomb composite	259
10.1.1 Introduction	259
10.1.2 Materials	262
10.1.3 Methodology	263
10.1.3.1 Fabrication of 3D woven honeycomb fabric	263
10.1.3.2 Production of the 3D woven honeycomb composite	266
10.1.3.3 Mechanical characterization	267
10.1.4 Results and Discussion	269
10.1.4.1 Flatwise compression	269
10.1.4.2 Edgewise compression	272
10.1.4.3 Three-point bending	275
10.2 Comparison of mechanical performance of FDM printed honeycomb structure with 3D woven honeycomb composite	280
10.2.1 Introduction	280
10.2.2 Materials	283
10.2.3 Methodology	284
10.2.3.1 Development of 3D printed ABS honeycomb structure by fused deposition modelling	284
10.2.3.2 Production of 3D woven honeycomb fabric	287

	<b>Page No.</b>
10.2.3.3 Production of 3D woven honeycomb composite	289
10.2.3.4 Mechanical characterization	290
10.2.4 Results and Discussion	290
10.2.4.1 Flatwise compression	290
10.2.4.2 Edgewise compression	293
10.2.4.3 Three-point bending	295
10.2.4.4 Low-velocity in-plane impact energy	297
10.2.5 Conclusions	299
<b>Chapter 11: Summary and Conclusions</b>	<b>301</b>
<b>Scope for future work</b>	<b>307</b>
<b>References</b>	<b>308</b>
<b>Publication details</b>	<b>350</b>
<b>Curriculum vitae</b>	<b>353</b>

## List of Figures

<b>Figures</b>	<b>Title</b>	<b>Page No.</b>
Figure 3.1	Types of three-dimensional cells (a) Tetrahedron (b) Triangular prism (c) Rectangular prism (d) Hexagonal prism (e) Octahedron (f) Rhombic dodecahedron (g) Pentagonal dodecahedron (h) Tetrakaidcahedron (i) Icosahedron	11
Figure 3.2	Mechanical response to compressive loading of stretch-dominated octet-truss unit cell	12
Figure 3.3	Two-dimensional honeycomb	14
Figure 3.4	Schematic illustration of honeycombs structure with different cell shape (a,b) Two packings of equilateral triangles (c,d) Two packings of squares (e) Packing of regular hexagon (f) Packing of irregular hexagon	15
Figure 3.5	Honeycomb core sandwich structure	16
Figure 3.6	Expansion manufacturing process	20
Figure 3.7	Corrugation manufacturing process	21
Figure 3.8	Equal uniform compression on two edges of rectangular cell wall	24
Figure 3.9	Classification of 3D woven fabrics based on weaves architecture (a) 3D woven 3D fabric (b) 2D woven 3D fabric	29
Figure 3.10	Classification of 3D woven fabrics based on the geometrical shape (a) 3D solid structures (b) 3D hollow structures (c) 3D profile structures	29
Figure 3.11	(a)Woven spacer fabric is integrally woven with a vertical pile yarn (b) vertical woven fabric between the outer fabric layers	32
Figure 3.12	Hollow structures formed by 2D honeycomb weave	33
Figure 3.13	Ordinary honeycomb weave	33

<b>Figures</b>	<b>Title</b>	<b>Page No.</b>
Figure 3.14	Construction of Brighton honeycomb weave (a) Insertion of single and double row(b) Complete Brighton honeycomb weave on 16 threads	34
Figure 3.15	A schematic diagram of woven fabric with multilayer structure (a) hexagonal shape (b) tetragonal shape	35
Figure 3.16	Stress distribution on honeycomb structure under bending load	39
Figure 3.17	Evolution of the equivalent plastic strain on the core during the simulation	41
Figure 3.18	Analysis of compression behavior of composite (Glass/epoxy) honeycomb structure	42
Figure 3.19	Honeycomb Directions	43
Figure 3.20	Honeycomb structure with hexagonal cells	44
Figure 3.21	A honeycomb carrying loads on the faces normal to $X_3$	48
Figure 3.22	Geometric parameters of honeycomb cell	49
Figure 3.23	Cross-section of an impact damaged sandwich plate	52
Figure 3.24	Description of the indentation test with a cylindrical indenter	53
Figure 3.25	Damaged honeycomb panels after impact tests ( $d = 3$ mm)	54
Figure 3.26	Collapse mode in bending	57
Figure 3.27	3D auxetic fabric sample	65
Figure 3.28	Sandwich panels with standard and auxetic cores and unit cell parameters	66
Figure 3.29	Local geometric unit cell sizing parameters	66
Figure 3.30	Hexagonal and re-entrant honeycombs using the Kirigami technique	67
Figure 4.1	Unit honeycomb cell	78

<b>Figures</b>	<b>Title</b>	<b>Page No.</b>
Figure 4.2	Cross-section representation of honeycomb structure 5P4L60 sample	79
Figure 4.3	Cross-section representation of 3D woven honeycomb fabric	80
Figure 4.4	Illustration of thickness of honeycomb structure	81
Figure 4.5	Customized rapier weaving machine	82
Figure 4.6	Image of VARIM process	85
Figure 4.7	Composite preparation (a)Preparation and insertion of moulds (b) composite sample after curing and removal of moulds	85
Figure 4.8	Experimental setup for flatwise compression test	86
Figure 4.9	Sandwich panel of 3D woven honeycomb composite for flatwise compression	87
Figure 4.10	Experimental setup for edgewise compression test	88
Figure 4.11	Composite specimen for edgewise compression	89
Figure 4.12	Experimental setup for three-bonding test	90
Figure 4.13	Experimental setup of impact test(a) drop-weight impact facility (b)close-up of hemispherical-nosed tup (c)Specimen fixture (d) Placement of sample for impact test	92
Figure 5.1	Lifting plans of 3D woven honeycomb fabric samples(a) 5P4L60 honeycomb (b) 7P4L60 honeycomb (c)(7,5)P4L60 honeycomb,(d) (5,3)P4L60 honeycomb and (e)(5,7)P4L60 honeycomb	98
Figure 5.2	Images of 3D woven honeycomb fabric sample (a) 5P4L60 honeycomb (b) 7P4L60 honeycomb (c)(5,3)P4L60 honeycomb,(d) (5,7)P4L60 honeycomb and (e)(7,5)P4L60 honeycomb	99
Figure 5.3	The repeat unit of the honeycomb structure	101
Figure 5.4	The unit hexagonal cell of the honeycomb	105

<b>Figures</b>	<b>Title</b>	<b>Page No.</b>
Figure 5.5	Measured and computed result for honeycomb fabric (a) Repeat unit weight (b) FVF (c) Specific weight	108
Figure 5.6	The predicted value for different value of wall length (a) Repeat unit weight (b) FVF (c) Specific weight	112
Figure 5.7	The predicted value for different picks in free wall length with constant picks in bonded wall length (a) repeat unit weight (b) FVF (c) specific weight	113
Figure 5.8	The predicted value for different picks in bonded wall length with constant picks in free wall length (a) repeat unit weight (b) FVF (c) specific weight	114
Figure 6.1	Schematic diagram of honeycomb samples with different cell sizes (a) 3P4L30 (b) 5P4L45 (c) 7P4L60 (d) 9P4L75	122
Figure 6.2	Schematic diagram of honeycomb samples with different opening angle (a) 5P4L30 (b) 5P4L45 (c) 5P4L60 (d) 5P4L75	123
Figure 6.3	Schematic diagram of honeycomb samples with different free wall length (a) (3,5) P4L60 (b) 5P4L60 (c) (7,5)P4L60 (d) (9,5)P4L60	123
Figure 6.4	Schematic diagram of honeycomb samples with different bonded wall length (a) (5,3)P4L60 (b) 5P4L60 (c) (5,7)P4L60 (d) (5,9)P4L60	124
Figure 6.5	Schematic diagram of honeycomb samples with different number of layers keeping cell shape constant (a) 5P3L60 (b) 5P4L60 (c) 5P5L60	124
Figure 6.6	Schematic diagram of honeycomb samples with different number of layers keeping composite thickness constant (a) 6P3L60 (b) 4P4L60 (c) 3P5L60	125
Figure 6.7	Lifting plans for different cell sizes	129
Figure 6.8	Lifting plans for different free wall length	130
Figure 6.9	Lifting plans for different bonded wall length	131

<b>Figures</b>	<b>Title</b>	<b>Page No.</b>
Figure 6.10	Lifting plans for different layers keeping cell shape constant	132
Figure 6.11	Lifting plans for different layers keeping composite thickness constant	133
Figure 6.12	3D woven honeycomb fabric sample (a) 5P4L60 honeycomb (b) 5P5L60 honeycomb (c)6P3L60 honeycomb(d) 7P4L60 honeycomb(e)(3,5)P4L60 honeycomb(f)(5,7)p4L60 honeycomb (g)(5,3)P4L60honeycomb and (h)(7,5)P4L60	135
Figure 6.13	Wooden block covered in Teflon sheet for use in composite construction	136
Figure 6.14	Composite structures of different cell size	136
Figure 6.15	Composite structures of different opening angle	136
Figure 6.16	Composite structures of different bonded wall length	137
Figure 6.17	Composite structures of different free wall length	137
Figure 6.18	Composite structures of different number of layers keeping cell shape constant	137
Figure 6.19	Composite structures of different number of layers keeping composite thickness constant	138
Figure 6.20	(a)2D woven fabric(b) 3D orthogonal weave design (c) 3D orthogonal fabric	139
Figure 6.21	(a)2D woven composite (b) 3D orthogonal composite	140
Figure 6.22	Schematic representation for the combination of face sheets	141
Figure 6.23	Sandwich panel of 3D woven honeycomb composite	142
Figure 6.24	Load deformation curve for different cell size in flatwise compression test	144
Figure 6.25	Compression energy of different cell sizes of the honeycomb in flatwise compression test (a) per unit weight (b) per unit volume	144

<b>Figures</b>	<b>Title</b>	<b>Page No.</b>
Figure 6.26	Load deformation curve for different opening angle in flatwise compression test	146
Figure 6.27	Compression energy of different opening angles of the honeycomb in flatwise compression test (a) per unit weight of (b) per unit volume	146
Figure 6.28	Load deformation curve for different free wall length in flatwise compression test	147
Figure 6.29	Compression energy of different free wall lengths of the honeycomb in flatwise compression test (a) per unit weight of (b) per unit volume	148
Figure 6.30	Load deformation curve for different bonded wall length in flatwise compression test	149
Figure 6.31	Compression energy of different bonded wall lengths of the honeycomb in flatwise compression test (a) per unit weight of (b) per unit volume	149
Figure 6.32	Load deformation curve for different number of layers keeping thickness constant in flatwise compression test	150
Figure 6.33	Compression energy of honeycomb for different number of layers keeping thickness constant in flatwise compression test (b) per unit weight of (c) per unit volume	151
Figure 6.34	Load deformation curve for different number of layers keeping cell shape constant in flatwise compression test	152
Figure 6.35	Compression energy of honeycomb for different number of layers keeping cell shape constant in flatwise compression test (a) per unit weight of (b) per unit volume	152
Figure 6.36	Load deformation curve for honeycomb core with thickened face sheet in flatwise compression test	154
Figure 6.37	Compression energy of honeycomb core with thickened face sheet in flatwise compression test (a) per unit weight of (b) per unit volume	154

<b>Figures</b>	<b>Title</b>	<b>Page No.</b>
Figure 6.38	Load deformation for honeycomb sample with different regimes in flatwise compression test	155
Figure 6.39	Buckling behavior in honeycomb during flatwise compression	156
Figure 6.40	(a), (b), and (c) Crushing behavior occurs in honeycomb after flatwise compression test	156
Figure 6.41	Load deformation curve for different cell sizes in edgewise compression test	158
Figure 6.42	Ultimate load of a honeycomb of different cell sizes in edgewise compression test (a) per unit weight (b)per unit volume	158
Figure 6.43	Load deformation curve for different opening angle in edgewise compression test	159
Figure 6.44	Ultimate load of a honeycomb of different opening angles in edgewise compression test (a) per unit weight (b)per unit volume	160
Figure 6.45	Load deformation curve for different free wall length in edgewise compression test	161
Figure 6.46	Ultimate load of a honeycomb of different free wall lengths in edgewise compression test(a) per unit weight (b) per unit volume	161
Figure 6.47	Load deformation curve for different bonded wall length in edgewise compression test	162
Figure 6.48	Ultimate load of honeycomb of different bonded wall length in edgewise compression test (a) per unit weight (b) per unit volume	163
Figure 6.49	Load deformation curve for different number of layers keeping cell size constant in edgewise compression test	164
Figure 6.50	Ultimate load of honeycomb of different number of layers keeping cell size constant in edgewise compression test(a) per unit weight (b) per unit volume	164
Figure 6.51	Load deformation curve for different number of layers keeping thickness constant in edgewise compression test	165

<b>Figures</b>	<b>Title</b>	<b>Page No.</b>
Figure 6.52	Ultimate load of honeycomb of different number of layers in edgewise compression test(a) per unit weight (b) per unit volume	166
Figure 6.53	Typical load – deformation curve of 3D woven honeycomb sandwich structure under the edgewise compression test	167
Figure 6.54	Cell deformation by elastic buckling: the elastic buckling occurs during edgewise compression of 3D woven honeycomb composites	168
Figure 6.55	Load deformation curve for different cell sizes in three-point bending test	169
Figure 6.56	Load of honeycomb with different cell sizes in three-point bending test(a) per unit weight (b) per unit volume	170
Figure 6.57	Load deformation curve for different opening angle in three-point bending test	171
Figure 6.58	Load of honeycomb with different opening angle in three-point bending test(a) per unit weight (b)per unit volume	171
Figure 6.59	Load deformation curve for different free wall length in three-point bending test	172
Figure 6.60	Load of honeycomb of different free wall length in three-point bending test(a) per unit weight (b) per unit volume	173
Figure 6.61	Load deformation curve for different bonded wall length in three-point bending test	174
Figure 6.62	Load of honeycomb of different bonded wall length in three-point bending test(a) per unit weight (b) per unit volume	174
Figure 6.63	Load deformation curve for different number of layers keeping cell size constant in three-point bending test	175
Figure 6.64	Load of honeycomb of different number of layers keeping cell size constant in three-point bending test(a) per unit weight (b) per unit volume	176

<b>Figures</b>	<b>Title</b>	<b>Page No.</b>
Figure 6.65	Load deformation curve for different number of layers keeping thickness constant in three-point bending test	177
Figure 6.66	Load of honeycomb for different number of layers in three-point bending test(a) per unit weight (b) per unit volume	177
Figure 6.67	Load deformation curve for honeycomb core with thickened face sheet in three-point bending test (a) per unit weight (b) per unit volume	179
Figure 6.68	Load of honeycomb for honeycomb core with thickened face sheet in three-point bending test (a) per unit weight (b) per unit volume	179
Figure 6.69	3D woven honeycomb composite (a)Typical Load-deformation curve (b)corresponding deformation in three-point bending test	181
Figure 6.70	Failure of the honeycomb specimen under three-point bending test	182
Figure 6.71	Collapse Mode 1 shown by (a)schematic representation (b) 3D woven honeycomb composite in three-point bending test	183
Figure 6.72	Honeycomb structure with different cell sizes subjected to 100J impact (a)Force-displacement curve and (b)Energy-time curve and (c)Specific energy absorption and (d) Damage fragmentation	185
Figure 6.73	Honeycomb structure with different opening angles subjected to 100J impact (a)Force-displacement curve and (b)Energy-time curve and (c)Specific energy absorption and (d) Damage fragmentation	186
Figure 6.74	Honeycomb structure with different free wall lengths subjected to 100J impact (a)Force-displacement curve and (b)Energy-time curve and (c)Specific energy absorption and (d) Damage fragmentation	188
Figure 6.75	Honeycomb structure with different bonded wall lengths subjected to 100J impact (a)Force-displacement curve and (b)Energy-time curve and (c)Specific energy absorption and (d) Damage fragmentation	190
Figure 6.76	Honeycomb structure with different number of layers keeping composite thickness constant subjected to 100J impact (a)Force-	191

<b>Figures</b>	<b>Title</b>	<b>Page No.</b>
	displacement curve and (b)Energy-time curve and (c)Specific energy absorption and (d) Damage fragmentation	
Figure 6.77	Honeycomb structure with different number of layers keeping cell shape constant subjected to 100J impact (a)Force-displacement curve and (b)Energy-time curve and (c)Specific energy absorption and (d) Damage fragmentation	193
Figure 7.1	Cell structural parameters of all honeycomb samples	199
Figure 7.2	Customized rapier weaving machine (a)Sisal honeycomb fabric(b)Kevlar honeycomb fabric	201
Figure 7.3	Lifting plans of honeycomb fabric samples (a) Glass fibre (b)Sisal fibre (c) Kevlar fiber	202
Figure 7.4	3D woven honeycomb fabric sample (a) Glass fibre (b)Sisal fibre (c)Kevlar fiber	203
Figure 7.5	3D woven honeycomb composites (a) glass fiber (b) sisal fiber (c)Kevlar fiber	203
Figure 7.6	Flatwise compression (a) Load-deformation curve (b) Compression energy per unit mass (c) Compression energy per unit volume of Glass, Kevlar and sisal honeycomb composite	205
Figure 7.7	Crushing behavior of honeycomb composite structures in flatwise compression (a)Glass fiber (b)Kevlar fiber and (c)Sisal fiber	206
Figure 7.8	Edgewise compression (a) Load-deformation curve (b) Ultimate load per unit mass (c) Ultimate load per unit volume of Glass, Kevlar and sisal honeycomb composite	207
Figure 7.9	Deformation of honeycomb composites during edgewise compression(a)Glass fiber (b)Kevlar fiber and (c)Sisal fiber	208
Figure 7.10	Three-point bending (a) Load-deformation curve (b) Ultimate load per unit mass (c) Ultimate load per unit volume of Glass, Kevlar and sisal honeycomb composite	209

<b>Figures</b>	<b>Title</b>	<b>Page No.</b>
Figure 7.11	Failure of the honeycomb specimen under three-point bending test (a)Glass fiber (b)Kevlar fiber (c)Sisal fiber honeycomb composite	210
Figure 7.12	(a)Force -displacement curve and (b)Energy-time curve and (c)Specific Peak energy and Specific total energy absorption in impact test of glass, Kevlar and sisal honeycomb composite	211
Figure 7.13	Damage fragmentation of honeycomb structure under in-plane impact test (a) glass fiber (b)Kevlar fiber (c)Sisal fiber honeycomb composite	212
Figure 8.1	Cross-sectional representation of different honeycomb structures of the unit cell (a) hexagonal (b)triangular (c)rectangular	215
Figure 8.2	Schematic representation of honeycomb structures of different cell shape:(a) Hexagon (b)Triangular (c) Rectangular structure	216
Figure 8.3	Lifting plans of honeycomb fabric samples (a) hexagon (HX) (b) triangular (TR) and (c) rectangular (RT)	219
Figure 8.4	Teflon-coated wooden block used for composite making	220
Figure 8.5	3D woven honeycomb composite (a) (a)regular hexagonal structure (HX) (b)triangular structure (TR) (c)rectangular structure (RT)	220
Figure 8.6	CAD model of honeycomb structure (a)regular hexagonal structure (b)triangular structure (c)rectangular structure	223
Figure 8.7	Load deformation curve for different cell structures for (a) flatwise compression (b)edgewise compression (c)three-point bending behavior (d) Force-displacement curve and (e)Energy-time curve for different cell structure honeycomb structure subjected to 100J impact	226
Figure 8.8	Compression energy of honeycomb of different cell structures for flatwise compression (a) per unit mass (b) per unit volume	227
Figure 8.9	The ultimate load of the honeycomb of different cell structures for edgewise compression (a) per unit mass(b) per unit volume	228

<b>Figures</b>	<b>Title</b>	<b>Page No.</b>
Figure 8.10	The ultimate load of the honeycomb of different cell structures for three-point bending (a) per unit mass (b) per unit volume	228
Figure 8.11	Specific Peak energy and Specific total energy absorption in impact test	229
Figure 8.12	Failure of honeycomb composites under flatwise compression (a) HX (b)TR (c)RT	230
Figure 8.13	Failure of honeycomb composites under edgewise compression (a) HX (b)TR (c)RT	230
Figure 8.14	Failure of honeycomb composites under three-point bending(a) HX (b)TR (c)RT	231
Figure 8.15	Damage fragmentation of honeycomb structure with different cell structure (a) HX (b)TR (c)RT	232
Figure 8.16	Meshed honeycomb composite structures (a)hexagonal structure (b)triangular structure (c)rectangular structure	233
Figure 8.17	Deformation pattern for (a)regular hexagonal structure (b)triangular structure (c)rectangular structure	233
Figure 8.18	Comparison of the load-deformation curve obtained from simulation and experimental work for (a) Hexagonal structure (HX) (b)Triangular structure (TR) (c)Rectangular structure (RT)	235
Figure 8.19	Comparison between simulated result and experimental result of compression energy/mass for different honeycomb cell structures	237
Figure 9.1	Cross-section representation of 3D woven honeycomb fabric	241
Figure 9.2	Cell structural parameter of warp and weft honeycomb sample	242
Figure 9.3	Weft way honeycomb fabric(a) Weaving direction perpendicular to warp threads (b)Lifting plan	245
Figure 9.4	Warp way honeycomb fabric(a) Weaving direction parallel to warp threads (b)Lifting plan	246

<b>Figures</b>	<b>Title</b>	<b>Page No.</b>
Figure 9.5	3D woven honeycomb fabric sample (a) Warp way honeycomb (b) weft way honeycomb	247
Figure 9.6	3D woven honeycomb composite (a)warp way honeycomb (b)weft way honeycomb	248
Figure 9.7	Flatwise compression (a) Load-deformation curve (b) Compression energy per unit mass (c) Compression energy per unit volume of warp and weft way honeycomb composite	250
Figure 9.8	Crushing behavior of honeycomb structure in flatwise compression (a)Warp way honeycomb composite (b)Weft way honeycomb composite	251
Figure 9.9	Edgewise compression (a) Load-deformation curve (b) Ultimate load per unit mass (c) Ultimate load per unit volume of warp and weft way honeycomb composite	252
Figure 9.10	Deformation of honeycomb during edgewise compression (a)Warp way honeycomb composite (b)Weft way honeycomb composite	253
Figure 9.11	Three-point bending (a) Load-deformation curve (b) Ultimate load per unit mass (c) Ultimate load per unit volume of warp and weft way honeycomb composite	254
Figure 9.12	Failure of the honeycomb specimen under three-point bending test (a)Warp way honeycomb composite (b)Weft way honeycomb composite	255
Figure 9.13	(a)Force-displacement curve (b)Energy-time curve and (c)Specific energy absorption of warp and weft way honeycomb composite in impact test	257
Figure 9.14	Damage fragmentation of honeycomb structure under impact test (a)Warp way honeycomb composite (b)Weft way honeycomb composite	257
Figure 10.1	(a)Aluminium alloy 3003 honeycomb(b) honeycomb cell structure	263
Figure 10.2	Customized rapier weaving machine	264

<b>Figures</b>	<b>Title</b>	<b>Page No.</b>
Figure 10.3	Lifting plan of 3D woven honeycomb Kevlar sample	265
Figure 10.4	3D woven honeycomb (a) fabric and (b) composite structure	266
Figure 10.5	(a) Experimental setup for flatwise compression test (b) Sandwich panel of honeycomb core with the core thickness of 20mm	267
Figure 10.6	Experimental setup for edgewise compression test	268
Figure 10.7	Experimental setup for three- point bending test	269
Figure 10.8	Flatwise compression (a) Load-deformation curve (b) Compression energy per unit mass (c) Compression energy per unit volume of Metal and Kevlar honeycomb sample	270
Figure 10.9	Crushing behavior of honeycomb structure in flatwise compression (a) Metal honeycomb sample (b) Kevlar woven honeycomb sample	272
Figure 10.10	Edgewise compression (a) Load-deformation curve (b) Ultimate load per unit mass (c) Ultimate load per unit volume of Metal and Kevlar honeycomb sample	274
Figure 10.11	Deformation of honeycomb during edgewise compression (a) Metal honeycomb sample (b) Kevlar woven honeycomb sample	275
Figure 10.12	Three-point bending (a) Load-deformation curve (b) Ultimate load per unit mass (c) Ultimate load per unit volume of Metal and Kevlar honeycomb sample	276
Figure 10.13	Collapse modes of honeycomb structure (a) Mode 1 (b) Mode 2	277
Figure 10.14	Failure of the honeycomb specimen under three-point bending test (a) Metal honeycomb sample (b) Kevlar woven honeycomb sample	278
Figure 10.15	3D printer for developing FDM printed honeycomb	284
Figure 10.16	(a) Honeycomb structure modelled in solid works (b) Honeycomb structure produced by FDM	286
Figure 10.17	Lifting plan of 3D woven glass honeycomb sample	288

<b>Figures</b>	<b>Title</b>	<b>Page No.</b>
Figure 10.18	3D woven glass honeycomb (a) fabric and (b)composite structure	290
Figure 10.19	Flatwise compression (a) Load-deformation curve (b) Compression energy per unit mass (c) Compression energy per unit volume of 3D printed and woven honeycomb sample	292
Figure 10.20	Crushing behavior of honeycomb structure in flatwise compression (a)3D woven honeycomb composite (b)3D printed honeycomb sample	292
Figure 10.21	Edgewise compression (a) Load-deformation (b) Ultimate load per unit mass (c) Ultimate load per unit volume of 3D printed and woven honeycomb sample	294
Figure 10.22	Deformation of honeycomb during edgewise compression (a)3D woven sample(b)3D printed sample	295
Figure 10.23	Three-point bending (a) Load-deformation curve (b) Ultimate load per unit mass (c) Ultimate load per unit volume of 3D printed and woven honeycomb sample	296
Figure 10.24	Failure of the honeycomb specimen under three-point bending test (a)3Dwoven honeycomb sample (b)3D printed sample	297
Figure 10.25	(a)Force -displacement curve and (b)Peak energy and total energy absorption of 3D printed and woven honeycomb sample in impact test	298
Figure 10.26	Damage fragmentation of honeycomb structure (a) front surface image of 3D woven honeycomb under impact test(b)rear surface image of 3D woven honeycomb (c)front surface image of 3D printed honeycomb (d)rear surface image of 3D printed honeycomb	299

## List of Tables

<b>Tables</b>	<b>Title</b>	<b>Page No.</b>
Table 3.1	Comparison between Aluminum, Nomex and Thermoplastic honeycomb	18
Table 3.2	The calculated value of Kc	27
Table 3.3	Comparison of metal honeycomb with woven honeycomb structure	69
Table 4.1	Mechanical properties of different fibers	73
Table 4.2	Properties of epoxy resin (LY556)	74
Table 4.3	Properties of hardener (Aradur HY 951)	75
Table 4.4	Mechanical Properties of ABS	76
Table 4.5	Properties of Aluminum honeycomb	77
Table 5.1	Structural parameters for 3D woven honeycomb fabric	100
Table 5.2	Three different characteristics of fabric namely repeat unit weight, FVF and specific weight were calculated by geometrical modeling	110
Table 6.1	Structural parameters of different honeycomb fabric	126
Table 6.2	Construction parameters of different layers of honeycomb	128
Table 6.3	Thickness of different face sheets	141
Table 7.1	Specification of individual fabric layers and construction parameters of glass, Kevlar and sisal fiber honeycomb	200
Table 9.1	Weaving specifications of warp and weft honeycomb	243
Table 10.1	Specification of individual fabric layers in E-Glass samples	265
Table 10.2	Cell structural parameters of honeycomb structure	266
Table 10.3	3D printing parameters of the honeycomb structure	286

<b>Tables</b>	<b>Title</b>	<b>Page No.</b>
Table 10.4	Cell structural parameters of the honeycomb structure	287
Table 10.5	Weaving parameters of glass woven honeycomb	289

## List of Abbreviations

---

<b>Abbreviation</b>	<b>Description</b>
FVF	Fiber volume fraction of honeycomb fabric
$S_{pw}$	Specific weight of honeycomb fabric
$W_{uc}$	Repeat unit weight of honeycomb fabric
VARIM	Vacuum assisted resin infusion method
FEM	Finite element modelling
1LFC	One layer face sheet
FDM	Fused Deposition Modeling
ABS	Acrylonitrile Butadiene Styrene
HX	Hexagonal honeycomb structure
TR	Triangular honeycomb structure
RT	Rectangular honeycomb structure
EPM	Ends per meter
PPM	Picks per meter
CAD	Computer Aided Design
ASTM	American Society for Testing and Materials

---